THE JOURNAL OF PHYSICAL CHEMISTRY B LETTERS

Published on Web 10/17/2007

Cyclodextrin-Based Self-Assembled Nanotubes at the Water/Air Interface

Jorge Hernández-Pascacio,[†] Cristina Garza,[‡] Xavier Banquy,[†,§] Norma Díaz-Vergara,[†] Alfredo Amigo,[£] Salvador Ramos,[‡] Rolando Castillo,[*,‡] Miguel Costas,[*,†] and Ángel Piñeiro[*,†]

Laboratorio de Biofisicoquímica, Departamento de Fisicoquímica, Facultad de Química, Universidad Nacional Autónoma de México, Cd. Universitaria, México D.F. 04510, México, Instituto de Física, Universidad Nacional Autónoma de México, P. O. Box 20-364 México, D. F. 01000, México, and Departamento de Física Aplicada, Facultad de Física, Universidad de Santiago de Compostela, E-15782, Santiago de Compostela, Spain

Received: August 15, 2007; In Final Form: September 21, 2007

Native α-cyclodextrin (α-CD) is found to spontaneously form films at aqueous solution/air interfaces. Shape-response measurements to volume perturbations on drops hanging from a capillary indicate that temperature and sodium dodecyl sulfate (SDS) concentration strongly modify the viscoelastic properties of such films. By using isothermal titration calorimetry (ITC), Brewster angle microscopy (BAM), atomic force microscopy (AFM), and molecular dynamics (MD) simulations, it is shown that the films consist of self-assembled nanotubes whose building blocks are cyclodextrin dimers (α-CD_2) and α-CD_2−SDS_1 complexes.

1. Introduction

Tubular assemblies have potential applications as closed reaction chambers, size-dependent filters for substrates, modifiers of chemical functionality and enzyme activity, and carriers of chemical information.[1] The use of classical carbon nanotubes is limited by their low solubility in polar solvents, a problem that has been addressed mainly through their functionalization.[2,3] As another alternative, synthetic and threaded cyclodextrin-based tubular assemblies have been designed,[4−9] taking advantage of the toroidal geometry and physicochemical properties of these cyclic oligosaccharides. Such structures have been found either in solution or deposited on solid surfaces. Technological applications of this kind of assemblies are still far from reality, and hence, more research on their behavior and properties is needed. Here, two types of self-assembled nanotubes that form films at the water/air interface are reported. Nanotubes of pure native α-cyclodextrin (α-CD) were found in aqueous solution, while the addition of the ionic surfactant sodium dodecyl sulfate (SDS) led to SDS-filled nanotubes that strongly enhanced the film viscoelasticity. The temperature also proved to importantly affect the mechanical properties of the film in a certain concentration range of both solutes. Overall, self-assembled tubular structures based on native α-CD, that is, with no chemical modification, and SDS demonstrate the ability to strongly modify the water/air interface behavior. Our work opens an avenue for designing new materials with technological applications, through the employment of other cyclodextrins and guest molecules.

2. Materials and Methods

The α-CD + water and α-CD + SDS + water mixtures were analyzed both in the bulk phase and at the water-solution/air interface by static and dynamic surface tension measurements, viscoelastic parameter determinations, isothermal titration calorimetry, Brewster angle microscopy, atomic force microscopy, and molecular dynamics simulations. Details are given in the Supporting Information.

3. Results and Discussion

Using a drop volume tensiometer, maximum drop volume (MDV) measurements of α-CD + SDS aqueous mixtures hanging from a capillary were performed from 283.15 to 323.15 K in a wide range of concentrations. At each temperature, normalized maximum drop volumes ($NMDV = (MDV)_{solution}/(MDV)_{water}$) were obtained (Figure 1a−c). Notably, for $r = [\alpha\text{-CD}]/[SDS] > 2$ and 283.15 K (Figure 1b−c), drop volumes are ∼23% bigger than those for water. Under equilibrium conditions, MDV would be proportional to surface tensions (γ) and hence would translate into γ values higher than those for water. For a mixture with $r = 2.34$, drops whose volumes are between the MDV of the sample itself and that for water are stable for long times, but they finally detach from the capillary (Figure 1d). The dynamic surface tension behavior of this sample is abnormal since it increases exponentially before the drop detaches from the capillary (Figure 1d). These findings suggest that the liquid/air interface properties of α-CD + SDS aqueous mixtures are related to the large NMDV values. To gain insight into this interface, drop shape responses to volume perturbations were measured (Figure 1e and drops images). For water drops (Figure 1f) and those of the binary mixtures (α-CD + water) and (SDS + water), drop vertical size response to a volume

* To whom correspondence should be addressed. E-mail: rolandoc@fisica.unam.mx (R.C.); costasmi@servidor.unam.mx (M.C.); fangel@servidor.unam.mx (Á.P.).

[†] Facultad de Química, Universidad Nacional Autónoma de México (UNAM).

[‡] Instituto de Física, Universidad Nacional Autónoma de México (UNAM).

[§] Present address: Faculty of Pharmacy, Université de Montréal, C.P. 6128 Succ. Centreville, Montréal, Québec, Canada H3C 3J7.

[£] Universidad de Santiago de Compostela.

10.1021/jp076576t CCC: $37.00

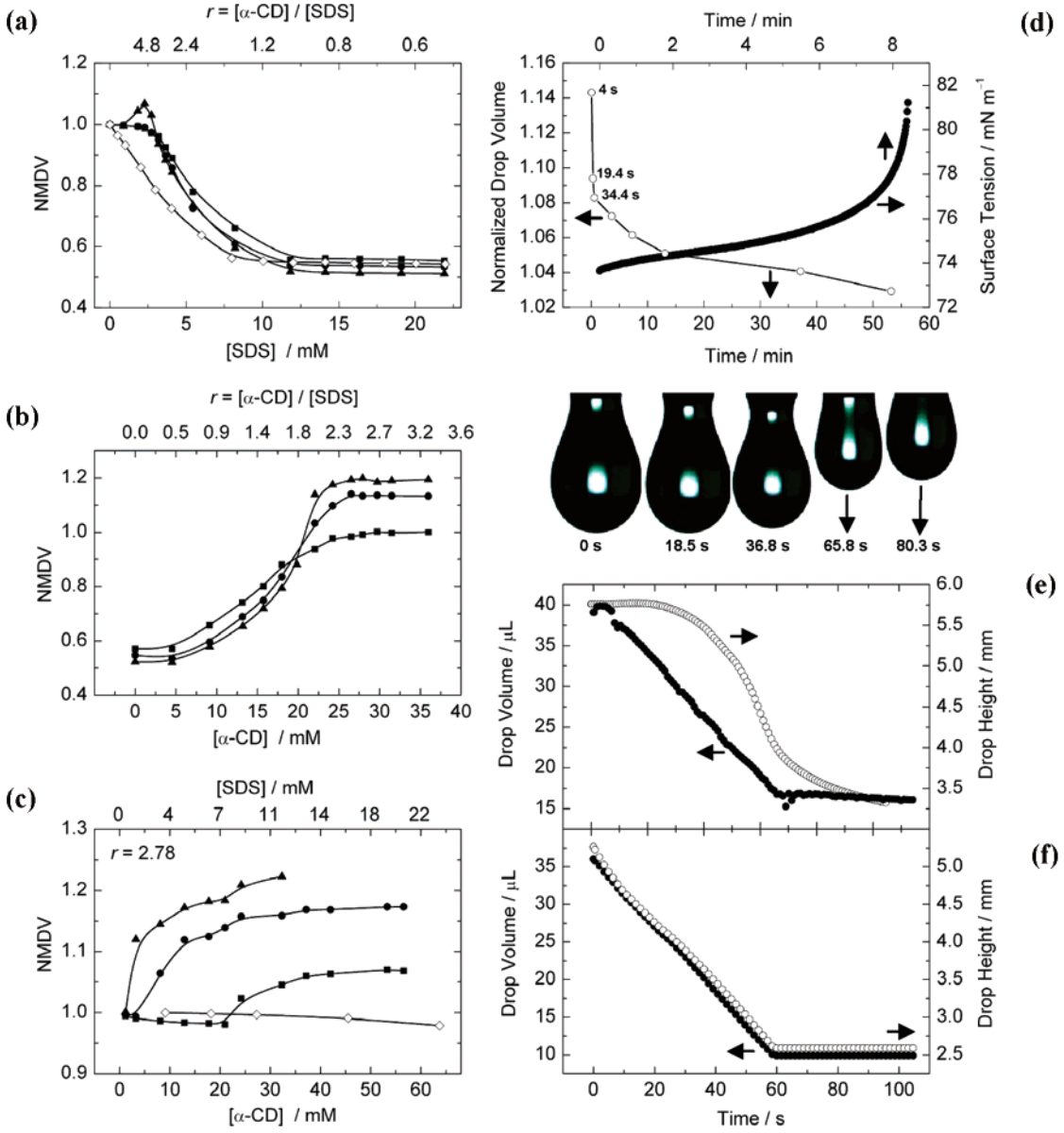

Figure 1. Normalized maximum drop volumes (NMDV) for α-CD + SDS + water mixtures at 283.15 (▲), 303.15 (●), and 323.15 K (■) at (a) constant α-CD concentration (12 mM), (b) constant SDS concentration (11 mM), and (c) constant r = [α-CD]/[SDS] = 2.78. Also shown are NMDV values (◇) at 303.15 K for SDS + water (a) and at 283.15 K for α-CD + water (c). Lines are only to aid visualization. At r = 2.34 and ~295 K, the elapsed time before a drop of constant volume (NDV) is detached from the capillary (○), with NDV being between MDV for pure water and MDV for this sample, and dynamic surface tensions (●) for a drop of ~1.06 NDV (d); dynamic drop height (○) while its volume (●) is reduced at a constant 0.405 μL s^{-1} rate (e), drop images at the indicated times being shown. The same experiment displayed in (e) was performed for pure water (f).

reduction is instantaneous, indicating that equilibrium is rapidly reached and hence NMDV values can be read as normalized surface tensions ($\gamma_{solution}/\gamma_{water}$). In contrast, a remarkable nonlinear delay was observed for α-CD + SDS aqueous mixtures with $r > 2$ (Figure 1e). As the shear viscosity of the ternary solution is only slightly higher than that of water, the nonlinear drop deformation response is due to its surface viscoelastic properties. By imposing a sinusoidal drop volume perturbation, the dilatational modulus of the surface at low frequencies (<0.1 Hz) was estimated to be 88.6 mN m^{-1}, approximately 40 times bigger than those of the binary mixtures. Then, addition of SDS to α-CD + water solutions drastically changed their liquid/air interface properties, producing a highly viscoelastic surface. This behavior can be modulated with SDS concentration and temperature. A surface whose viscoelastic properties can be modified with the addition of a cosolute has potential applications; it is also interesting by itself from the physicochemical point of view and deserves further examination. In what follows, a detailed characterization of this system at different levels is provided.

The NMDV rise (Figure 1b) when α-CD is added to a SDS + water mixture is due to a depletion of surfactants from the surface to the bulk liquid,[10] the SDS molecules being sequestered by α-CD molecules to form inclusion complexes.[11] To characterize these complexes, ITC measurements were performed from 283.15 to 308.15 K. The analysis of the data (see Figure S1 in Supporting Information) indicates that the species α-CD_1−SDS_1 and α-CD_2−SDS_1 coexist in equilibrium in the bulk liquid. Application of a sequential binding sites model[12] provided the equilibrium constants for the formation of each inclusion complex. At 283.15 K, K_{11} = 14400 ± 900 M^{-1} and K_{21} = 87800 ± 5400 M^{-1}; at 308.15 K, K_{11} = 16200 ± 300 M^{-1} and K_{21} = 7800 ± 200 M^{-1}. Thus, at low temperatures, the α-CD_2−SDS_1 complex is the predominant species in the bulk liquid

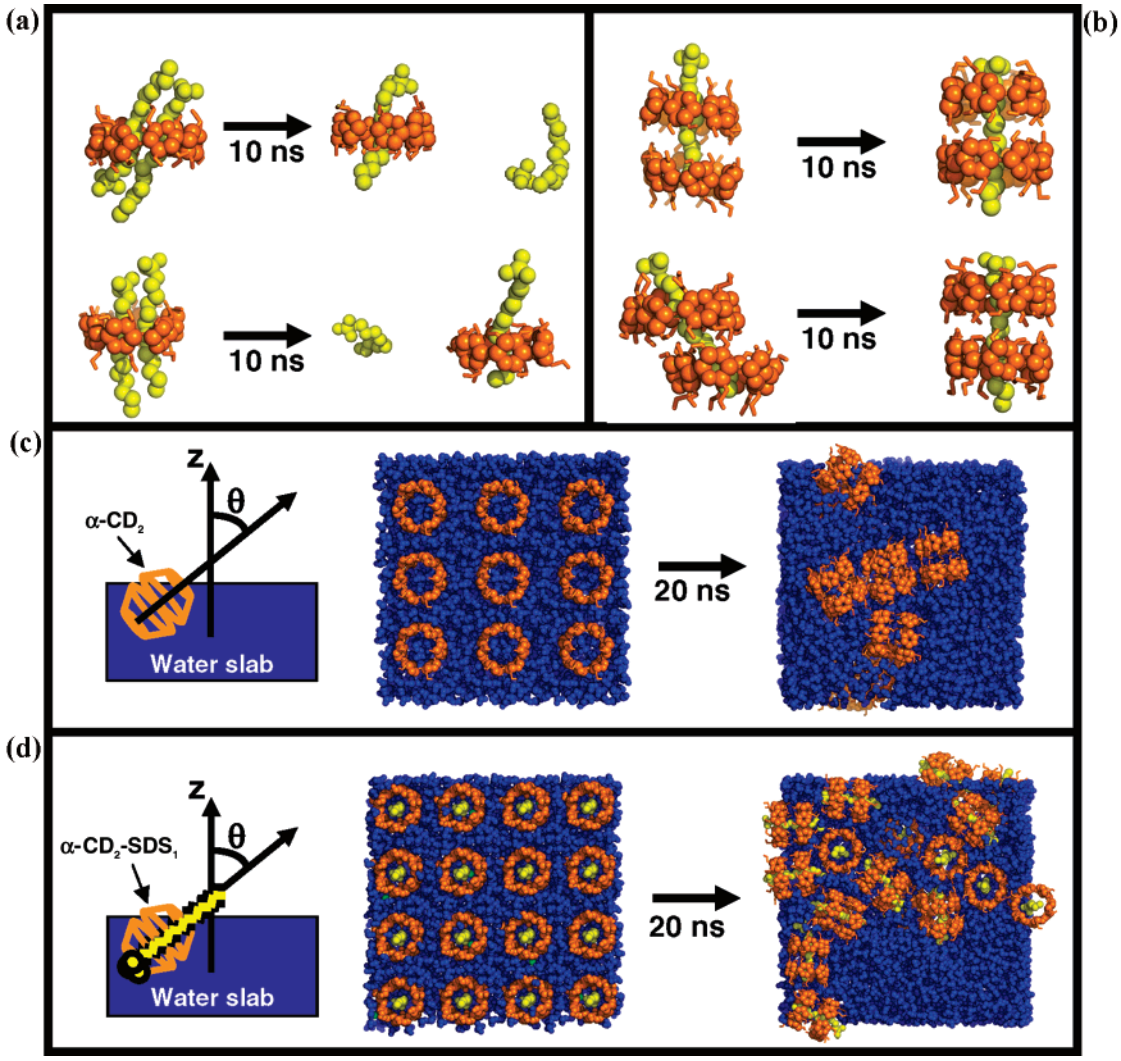

Figure 2. Initial (left) and final (right) structures from molecular dynamics trajectories. The starting conformations were α-CD_1−SDS_2 (a) and α-CD_2−SDS_1 (b) in the bulk liquid at 298 K and α-CD dimers (c) and α-CD_2−SDS_1 complexes (d) at the water/air interface and 283 K with $\theta = 0°$. The top views in (c) and (d) show that the dimers (c) and most complexes (d) are stable at the interface and rotate to $\theta = 90°$. Other dimers and complexes immerse themselves in the bulk liquid. The time scales for each simulation are indicated, and θ is defined in (c) and (d).

mixture. This ITC result together with the NMDV measurements for $r > 2$ strongly suggests that the α-CD_2−SDS_1 complexes are surface-active and are involved in the behavior of this system (Figure 1).

In agreement with the ITC results, MD simulations starting from 14 different conformations for the α-CD/SDS complexes (Figure S7) indicate that the 1:1 and 2:1 complexes are present in the bulk (Figure 2a and b). The same stoichiometries have been recently observed for α-CD with a carbohydrate surfactant.[12] In the structure obtained for the 2:1 complex (Figure 2b), the hydrophobic tail of the SDS molecule was simultaneously present in both α-CD cavities, and the two cyclodextrin molecules faced each other by the wider side of their original truncated cone shape, in agreement with scanning tunneling microscopy results for α-CD necklaces.[9] Upon complexation, both α-CD molecules switched to a cylindrical geometry and were bridged, on average, by 9−10 H bonds formed between the hydroxyl groups located at the edge of the cone. MD simulations for the α-CD_2 dimer without SDS produced a stable structure with the same relative orientation of the CD molecules. The inclusion of the SDS molecules is an additional stabilization factor over the intermolecular α-CD/α-CD H bonds.

The presence of assemblies at the solution/air interface was observed using BAM. First, observations were performed for the α-CD + water mixture (Figure 3a and b). BAM images demonstrate that although α-CD is not surface-active (Figure 1c), cyclodextrin molecules are present at the liquid/air interface in large quantities, forming a film with a variety of self-assembled complex domains. These molecular arrangements are capable of incorporating themselves into the water surface network in such a way that there is almost no change of surface energy. BAM images for α-CD + SDS + water mixtures, all with $r = 2$ (Figure 3c and d), show that the presence of SDS produces a smoother and rigid (not fluid) film that must be responsible for the atypical liquid/air interface properties (Figure 1).

ITC and MD results suggest that α-CD_2 and α-CD_2−SDS_1 species are the basic units of the films observed by BAM. This prompted MD simulations at the water/air interface. α-CD dimers were initially oriented with $\theta = 0°$, θ being the angle between the α-CD symmetry axis and the perpendicular to the interface plane. At 283 K, most of the dimers rotated to $\theta = 90°$ after a few nanoseconds and remained at the surface, keeping their cylindrical geometry (Figure 2c). As in the bulk phase, intermolecular H bonds were responsible for the stabilization of the dimer structure. For the α-CD + SDS + water system, α-CD_2−SDS_1 complexes were initially placed with $\theta = 0°$ and the SDS ionic head oriented toward the interior of

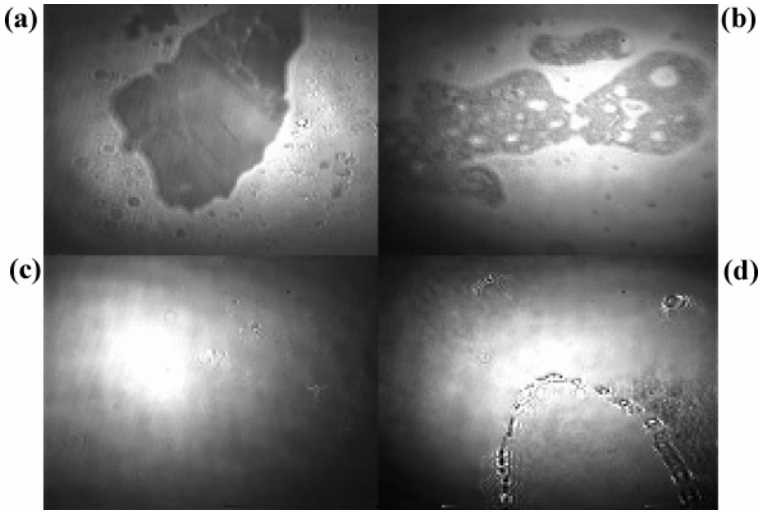

Figure 3. Brewster angle microscopy images of the solution/air interface at a resolution of 4 μm. For α-CD + water at 35 mM and 283 K (a), a film with many defects is clearly observed. Domains of different brightness indicate a nonconstant film thickness. Defects such as openings and islands clustered in small regions with different thicknesses are also visible. At low concentration (2.5 mM) and higher temperature (303 K) (b), the film appears to be more fluid, and apparently, two phases are coexisting. For α-CD + SDS + water at [α-CD] = 35 mM and [SDS] = 17.5 mM ($r = 2$) and 286 K (c), a smooth rigid film is formed along the entire liquid/air interface. At lower α-CD (5 mM) and SDS (2.5 mM) concentrations ($r = 2$) and 285 K (d), the film presents defects but remains rigid. Movies of these BAM observations are available upon request.

the bulk liquid. As with the α-CD_2, many of the complexes rotated to $\theta = 90°$ (Figure 2d).

MD simulations were also performed to gain insight into the supramolecular arrangements that, having α-CD_2 and α-CD_2−SDS_1 as basic units, produce the films observed by BAM. For the binary mixture, three series of simulations at 283 K were performed starting from the arrangements of (i) a single tube constituted by four units, $(\alpha\text{-}CD_2)_4$, (ii) two $(\alpha\text{-}CD_2)_4$ tubes placed next to each other (Figure S8), and (iii) two and three layers of $(\alpha\text{-}CD_2)_4$ tubes (Figures 4a and S9), all of them placed over the water/air interface with $\theta = 90°$. In a few hundred picoseconds, all of the tubes partially immersed themselves in the water interface structure and thereafter remained stable. The final conformations (after 20 ns) indicate that, within each tube, there are water molecules bridging the α-CD_2 dimers (Figure 4b). The structure of each dimer preserves the direct H bonds between cyclodextrins. For (ii) and (iii), the tubes approached each other, keeping water channels between them. An additional two-layer simulation starting with $\theta = 0°$ showed that the α-CD_2 dimers progressively tilted to 45° during a 10 ns trajectory (Figure S10). This suggests that the final conformations obtained starting from $\theta = 90°$ are not artifacts. It appears that the fractured films of different thicknesses observed by BAM were formed by $(\alpha\text{-}CD_2)_n$ tube multilayers at the water/air interface. In this self-assembled structure, H bonds provide the major contribution to the surface energy, as in pure water surface. This would explain the small difference between surface tension values of pure water and the α-CD + water mixture (Figure 1c). For the ternary system, due to the presence of the SDS ionic head, each α-CD_2−SDS_1 unit was treated as a dipole. Simulations at 283 K were performed starting from four α-CD_2−SDS_1 complexes with a different orientation of the dipoles (Figures S11 and S12) and two layers each with four $(\alpha\text{-}CD_2\text{−}SDS_1)_4$ tubes (Figures S13 and S14). The stable conformations were those with the α-CD_2−SDS_1 complexes with $\theta = 90°$, with the SDS molecules orientated in the same direction within each tube and in the opposite direction in the contiguous tube. Since a classical nonpolarizable force field was used (see the Methods section in Supporting Information), the dipole−dipole interactions did not have their origin in the polarizability of single ions[13,14] but in the distributions of charges within the molecules and of ions (sulfate and sodium). The single $(\alpha\text{-}CD_2\text{−}SDS_1)_4$ tube was not stable, but the α-CD_2−SDS_1 basic units remained at the surface with $\theta = 90°$. The behavior of the $(\alpha\text{-}CD_2\text{−}SDS_1)_4$ mono- and multilayers (Figure 4e and f) was the same as that for the $(\alpha\text{-}CD_2)_4$ tubes described above. An additional two-layer simulation starting from $(\alpha\text{-}CD_2\text{−}SDS_1)_2$ tubes with $\theta = 0°$ showed that the α-CD_2−SDS_1 dimers that remained at the interface tilted to 90° during a 30 ns trajectory (Figure S15). As compared with $(\alpha\text{-}CD_2)_4$ tubes, the dipole−dipole interactions between neighboring $(\alpha\text{-}CD_2\text{−}SDS_1)_4$ tubes (Figure 4e and f), as well as the electrostatic interactions arising from the presence of SDS and sodium ions, are additional factors determining the stability of the self-assembled supramolecular arrangements.

The structure of the SDS/α-CD self-assemblies at the liquid/air interface was explored using AFM experiments (see Methods section and Figures S2 and S3 in Supporting Information). Binary and ternary solutions were transferred to mica sheets, raising them from the solutions at 284 K using a Langmuir−Blodgett dipper, and subsequently dried. The self-assemblies attained under these conditions are assumed to be comparable to those occurring at the liquid/air interface. The homogeneous multilayered films were surveyed at room temperature using contact mode AFM. Force and topographic images for the binary (Figure 4c and d) and ternary (Figure 4g and h) mixtures show stripes with protruding bumps. Different scanning angles and consecutive amplifications preserve image features, ruling out artifacts (Figures S4 and S5). Also, measurements were repeated for different samples (Figure S6). In these complex architectures, the bump-to-bump distance along a stripe is 6.0 ± 0.5 Å, while the distance between bumps in parallel stripes is 5.2 ± 0.5 Å. The MD simulations (Figure 4b and f) suggest that each bump (Figure 4c, d, g, and h) is a glucopyranoside ring in an α-CD molecule. The individual atoms in these rings could not be resolved by the AFM tip. Since only two adjacent glucopyranosides per α-CD are accessible to the AFM tip, two parallel stripes comprise a tube constituted by α-CD_2 or α-CD_2−SDS_1 units. From the topographic AFM images, the films thicknesses were estimated to be at least 30 and 2 nm for the α-CD + SDS + water and the α-CD + water systems, respectively.

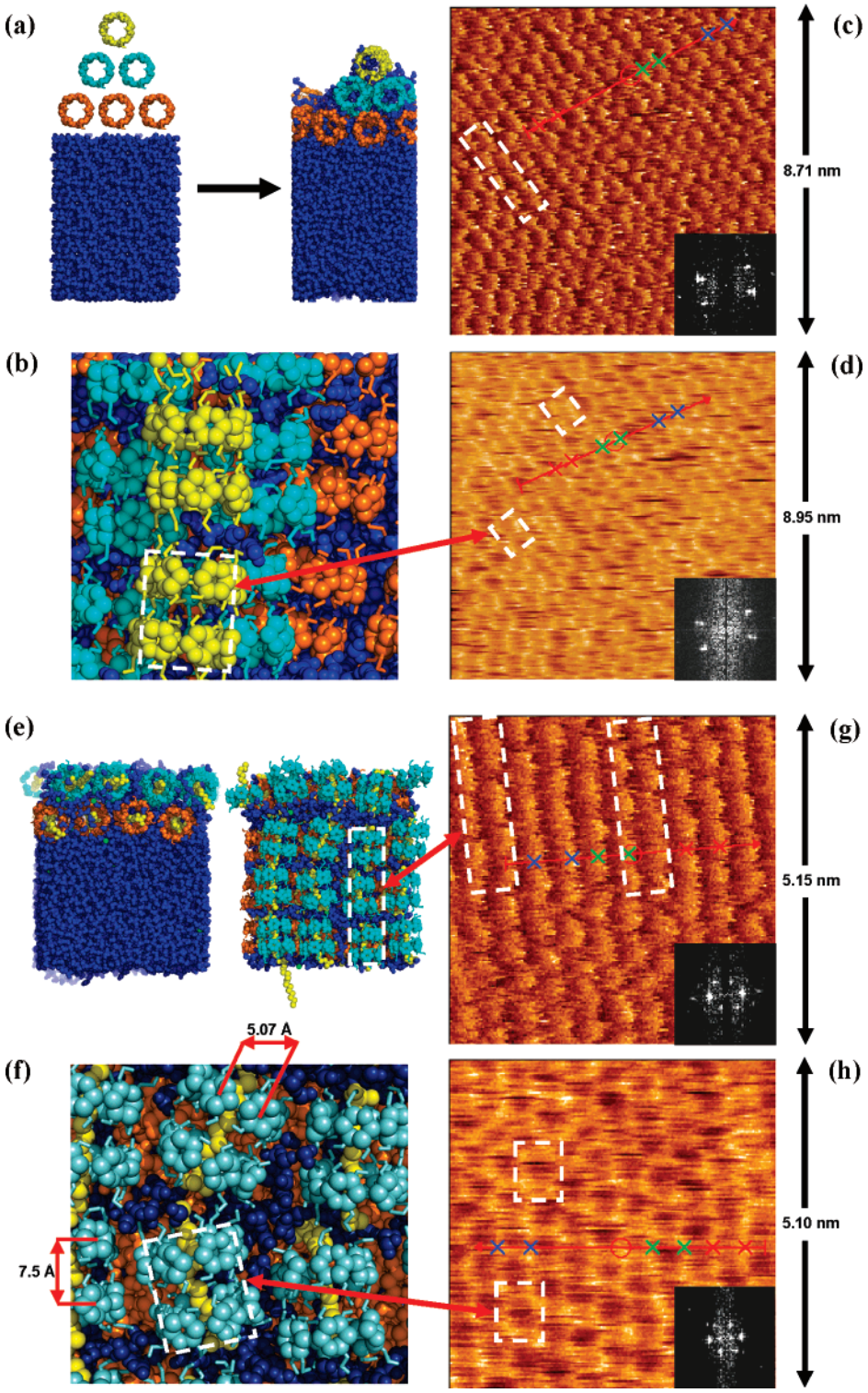

Figure 4. Structures from molecular dynamics trajectories at 283 K (left), force and topographic atomic force microscopy images of dried specimens (right) for α-CD + water (a−d) and α-CD + SDS + water (e−h), and fast Fourier transforms (insets in c, d, g, and h). Multilayers were transferred to freshly cleaved mica at 284 K and observed at room temperature. (a) Lateral views of six $(\alpha\text{-CD}_2)_4$ tubes for the initial (left) and final (right) conformations after a 20 ns simulation. (b) Amplified top view of the final conformation in (a). (e) Lateral (left) and top (right) views of the final conformation after a 20 ns simulation for two layers each with four $(\alpha\text{-CD}_2{-}\text{SDS}_1)_4$ tubes. (f) Amplified top view of the final conformation in (e). Force (c and g) and topographic (d and h) AFM images. Distances (±0.7 Å) between colored crosses (red, green, blue) are (c) 5.04, 5.27, 5.60 Å, (d) 5.69, 4.95, 5.57 Å, (g) 5.30, 4.76, 5.93 Å, and (h) 4.99, 4.81, 5.03 Å. The dashed white boxes enclose segments of $(\alpha\text{-CD}_2)_n$ tubes with $n = 4$ (c), $\alpha\text{-CD}_2$ units (b and d), $(\alpha\text{-CD}_2{-}\text{SDS}_1)_n$ tubes with $n = 3$ (e and g), and $\alpha\text{-CD}_2{-}\text{SDS}_1$ units (f and h).

4. Conclusions

The $(\alpha\text{-CD}_2)_n$ and $(\alpha\text{-CD}_2{-}\text{SDS}_1)_n$ are nanotubes self-assembled at the water/air interface, the later being reminiscent of cyclodextrin necklaces[9] but with a noncontinuous thread. The $(\alpha\text{-CD}_2)_n$ tubes are stable at the liquid/air interface due to H bond short-range interactions. The inclusion of SDS into the $\alpha\text{-CD}_2$ building blocks adds a stabilizing long-range interaction, producing a multilayer of orientated $(\alpha\text{-CD}_2{-}\text{SDS}_1)_n$ nanotubes. Such electrostatic cooperative interactions at the water/air

interface cause the remarkable viscoelastic behavior of this system. The results show that by using $(\alpha\text{-}CD_2)_n$ as a basic matrix, it is possible to devise systems with unique mechanical surface properties. The employment of different cyclodextrins and guest molecules opens an avenue for designing new materials with technological applications.

Acknowledgment. We are grateful to C. Knobler from the University of California, Los Angeles, D. Tobias from the University of California, Irvine, A. E. Mark from the University of Queensland, A. Martínez from IIM-UNAM, J. Arenas from IF-UNAM, and J. Gracia-Fadrique from FQ-UNAM for useful discussions. This work was supported by Grants 41328-Q, 46778-F, and J49811-Q from CONACyT, México, Grants IN110505 and IN105107 from PAPIIT-UNAM, México, Grant PGIDIT05PXIB20601PR from Xunta de Galicia, and Grant FIS2007-63479 from MEC, Spain. We thank Dirección General de Servicios de Cómputo Académico (DGSCA) of Universidad Nacional Autónoma de México (UNAM) and CESGA (USC) for computer time and for their excellent services. J.H-P. and N.D-V. are grateful for financial support from cátedra Raúl Cetina Rosado (Facultad de Química-UNAM) and CONACyT, respectively. J.H.-P. and C. G. contributed equally to this work.

Supporting Information Available: Materials and Methods section and Figures S1−S15. This material is available free of charge via the Internet at http://pubs.acs.org.

References and Notes

(1) Bong, D. T.; Clark, T. D.; Granja, J. R.; Ghadiri, M. R. *Angew. Chem., Int. Ed.* **2001**, *40*, 988−1011.
(2) Liu, Y. T.; Zhao, W.; Huang, Z. Y.; Gao, Y. F.; Xie, X. M.; Wang, X. H.; Ye, X. Y. *Carbon* **2006**, *44*, 1613−1616.
(3) Zeng, L. L.; Zhang, L.; Barron, A. R. *Nano Lett.* **2005**, *5*, 2001−2004.
(4) Harada, A.; Li, J.; Kamachi, M. *Nature* **1992**, *356*, 325−327.
(5) Harada, A.; Li, J.; Kamachi, M. *Nature* **1993**, *364*, 516−518.
(6) Harada, A.; Li, J.; Kamachi, M. *Nature* **1994**, *370*, 126−128.
(7) Li, G.; McGown, L. B. *Science* **1994**, *264*, 249−251.
(8) Zhang, C.; Shen, X.; Hongcheng, G. *Chem. Phys. Lett.* **2002**, *363*, 515−522.
(9) Miyake, K.; Yasuda, S.; Harada, A.; Sumaoka, J.; Komiyama, M.; Shigekawa, H. *J. Am. Chem. Soc.* **2003**, *125*, 5080−5085.
(10) Dharmawardana, U. R.; Christian, S. D.; Tucker, E. E.; Taylor, R. W.; Scamehorn, J. F. *Langmuir* **1993**, *9*, 2258−2263.
(11) Rekharsky, M. V.; Inoue, Y. *Chem. Rev.* **1998**, *98*, 1875−1917.
(12) Piñeiro, Á.; Banquy, X.; Perez-Casas, S.; Tovar, É.; García, A.; Villa, A.; Amigo, A.; Mark, A. E.; Costas, M. *J. Phys. Chem. B* **2007**, *111*, 4383−4392.
(13) Jungwirth, P.; Tobias, D. J. *J. Phys. Chem. B* **2001**, *105*, 10468−10472.
(14) Jungwirth, P.; Tobias, D. J. *Chem. Rev.* **2006**, *106*, 1259−1281.